

## Supporting Information

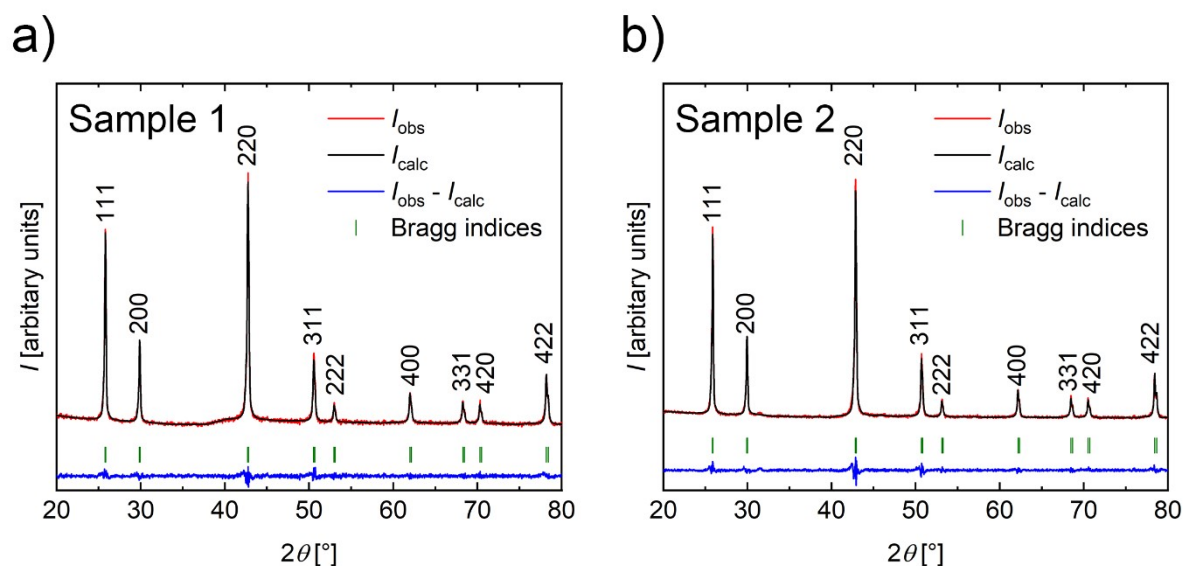


Figure S1: Rietveld refinements of sample 1 (a) and sample 2 (b) XRD diffraction patterns. Sample 2 might have a very small peak around 31.5 degrees which could be a peak that corresponds to the impurity phase.

Table S1: Rietveld refinement of  $\text{Mg}_2\text{VNi}_3\text{Sb}_3$  XRD diffraction patterns. Background points were manually selected and refined. Refined parameters are zero-point shift, scale factor, lattice parameter, peak shape (Pseudo-Voigt) and peak asymmetry parameters, and overall temperature factor. Atomic site occupancies were kept constant with mixed occupancy of Mg: V in the ratio 0.66667:0.33333 in the 4b site (1/2,1/2,1/2).  $\lambda_{\text{Cu-K}\alpha 1} = 1.54059 \text{ \AA}$ ,  $\lambda_{\text{Cu-K}\alpha 2} = 1.544310 \text{ \AA}$ .

Sample	$a$ [Å]	$\chi^2$	$R_{\text{Bragg}}$	$R_{\text{F}}$
1	5.9846(3)	1.20	1.51	0.942
2	5.9689(3)	1.65	2.24	1.50

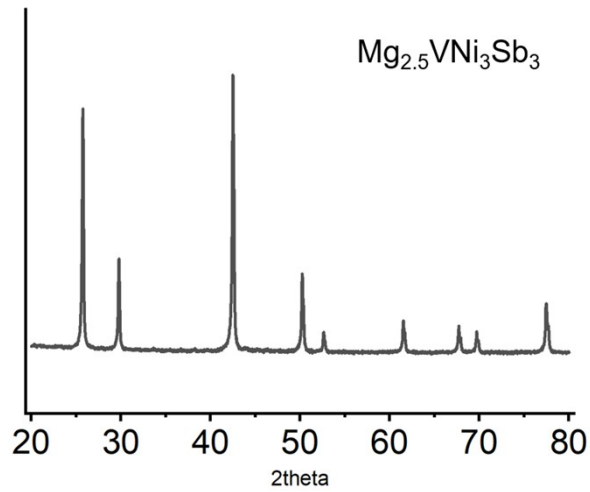


Figure S2: XRD diffraction patterns of  $\text{Mg}_{2.5}\text{VNi}_3\text{Sb}_3$ . All peaks were identified as half-Heusler peaks and no impurity peaks were detected in our measurement set up.

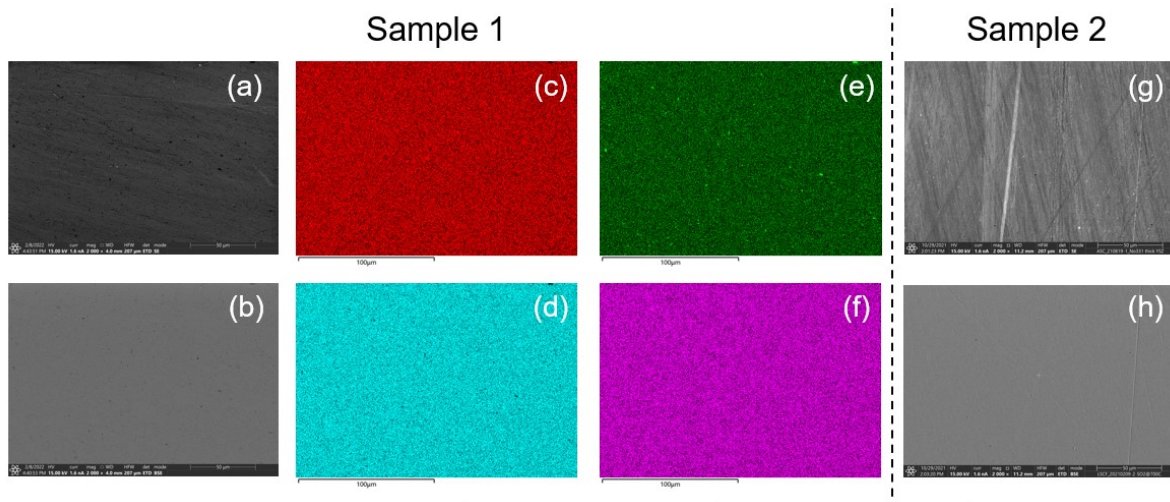


Figure S3: SEM (a, g), BSE (b, h), EDS mapping (c-f) of sample 1 (a-f) and 2 (g and h) showing the homogeneous compositional distribution of Mg, V, Sb, and Ni indicating the successful synthesis of the pure  $\text{Mg}_2\text{VNi}_3\text{Sb}_3$  phase. Small size V-rich precipitate might exist as the secondary phase as shown in (e). Microstructure analysis was performed by SEM (Thermo Fisher Scientific, Helios 5 Hydra DualBeam).

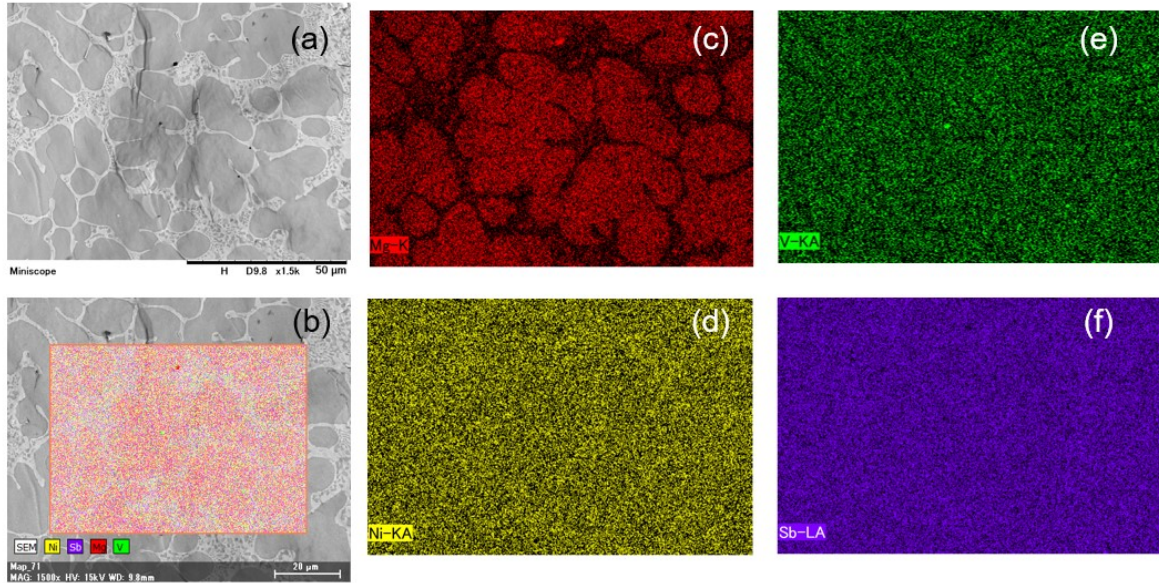


Figure S4: Microscopic data of sample 3. BSE image (a) shows the contrast in light gray and dark gray which corresponds to the compositional differences in Mg as shown in EDS mapping (b-f). The microstructure data were examined using scanning electron microscopy (SEM; 15 kV, Miniscope TM 3030Plus, Hitachi high-Technologies) coupled with energy-dispersive X-ray spectroscopy (EDX; Quantax 70, Bruker).

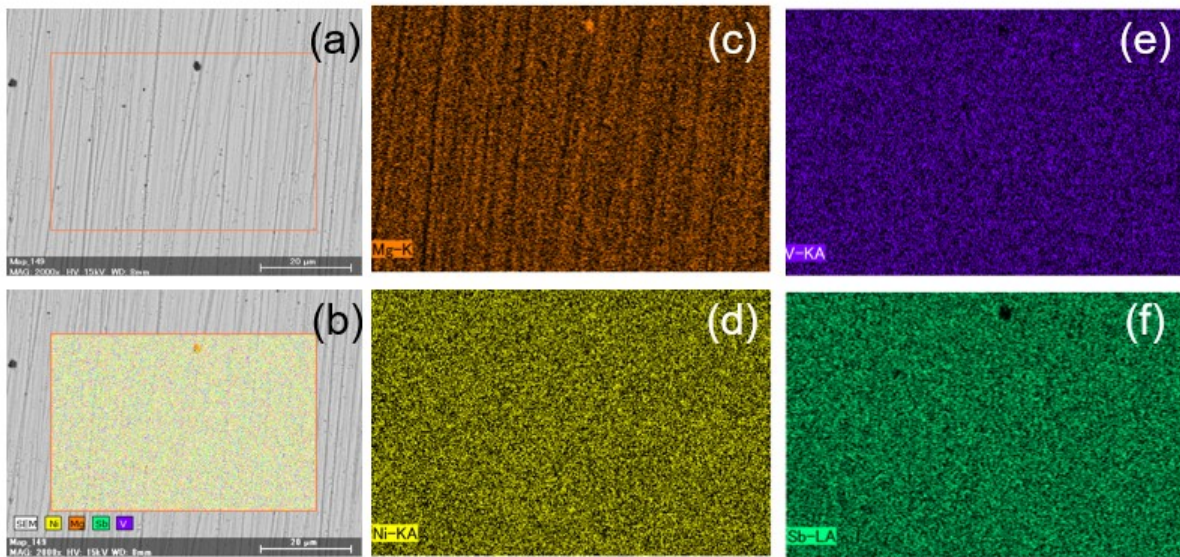


Figure S5: Microscopic data of  $\text{Mg}_{2.5}\text{VNi}_3\text{Sb}_3$ . BSE image (a) and EDS mapping (b-f) showed a relatively homogeneous matrix phase while there are small amount of Mg-rich precipitate as shown in Mg elemental mapping result (c). The microstructure data were examined using scanning electron microscopy (SEM; 15 kV, Miniscope TM 3030Plus, Hitachi high-Technologies) coupled with energy-dispersive X-ray spectroscopy (EDX; Quantax 70, Bruker). Average elemental composition obtained from EDS is Mg:V:Ni:Sb=30.08:10.35:28.14:31.43 that were more Mg-rich than sample 2.

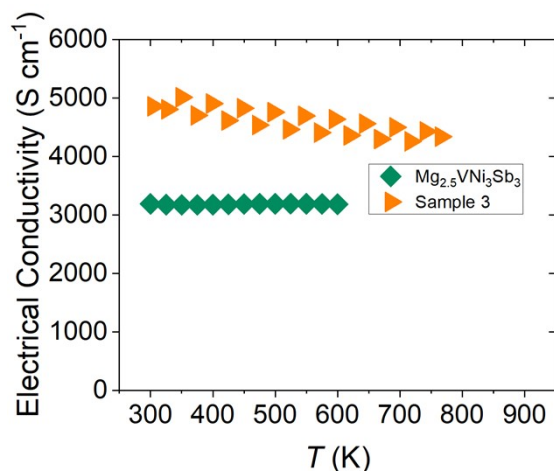


Figure S6 □ Electrical conductivity of  $\text{Mg}_2\text{VNi}_3\text{Sb}_3$  (sample 3) and  $\text{Mg}_{2.5}\text{VNi}_3\text{Sb}_3$ .

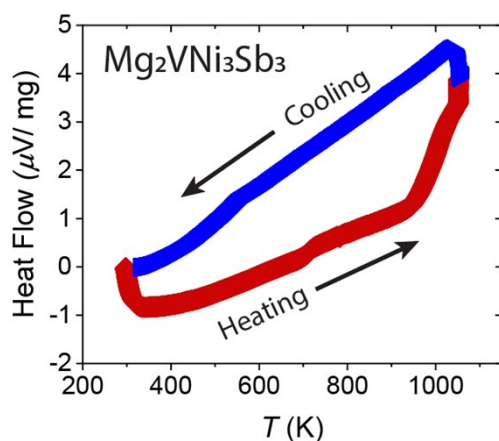


Figure S7 □ DTA result. There is no noticeable peak or change in heat flow indicating it is stable (no phase transition, decomposition, etc.) in this temperature range.

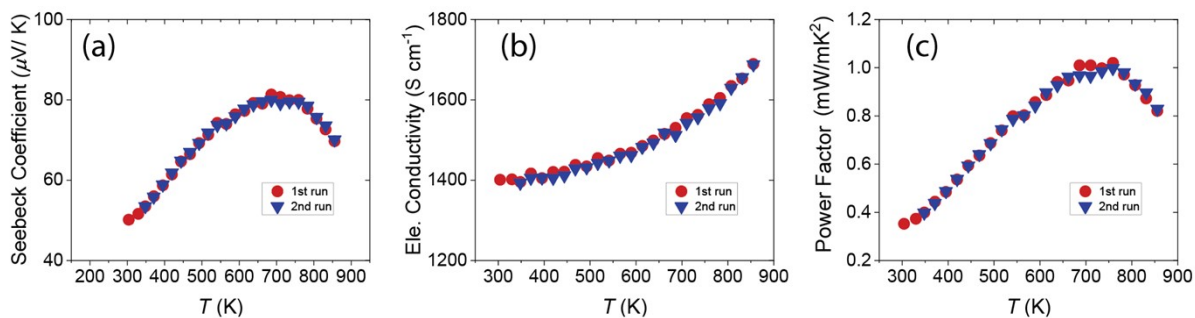


Figure S8 □ (a) Seebeck coefficient, (b) electrical conductivity, and (c) power factor of  $\text{Mg}_2\text{VNi}_3\text{Sb}_3$  (sample1) of 2 consecutive measurements. No hysteresis or changes were observed indicating the stability of this compound up to the measurement temperature of 873K.

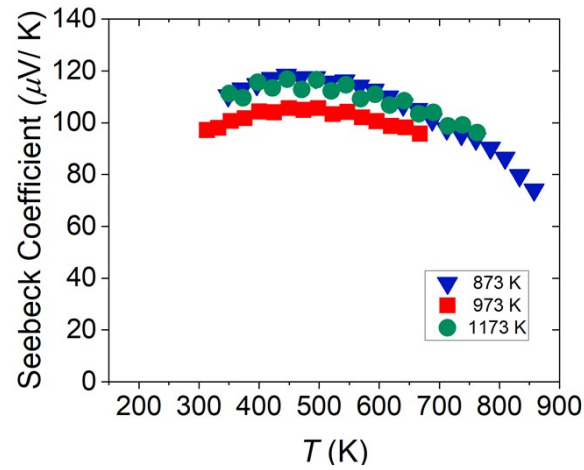


Figure S9 □ Reproducibility of the sample.  $\text{Mg}_2\text{VNi}_3\text{Sb}_3$  (sample 2) with 3 different pressing temperature (873 K, 973 K, 1173 K) provided similar Seebeck coefficients which are larger than  $100 \mu\text{V K}^{-1}$ .